Crystallization of Metallocene-Made Isotactic Polypropylene: Disordered Modifications Intermediate between the α and γ Forms

Finizia Auriemma* and Claudio De Rosa

Dipartimento di Chimica, Università di Napoli "Federico II", Complesso Monte S. Angelo, Via Cintia, 80126 Napoli, Italy

Received April 25, 2002; Revised Manuscript Received August 12, 2002

ABSTRACT: A detailed analysis of the structure and the thermal behavior of samples of isotactic polypropylene (iPP) prepared with a highly regiospecific metallocene catalysts is presented. The samples present variable amounts of stereodefects (isolated rr triads) and provide the first example of metallocene-made iPP not including regioirregularities. They crystallize from the melt in mixtures of the α and γ forms. The content of the γ form increases with increasing the crystallization temperature, reaches a maximum value, and then decreases for a further increase of the temperature. The crystallization of the γ form is favored by the presence of stereodefects. The thermal analysis has indicated that the crystals of γ form melt at lower temperature than the crystals of α form obtained at the same crystallization temperature. A comparison between the experimental X-ray diffraction profiles of the melt-crystallized samples and the calculated profiles for models of structure has shown that the γ form obtained in these samples always presents structural disorder, which produces local situation of packing typical of the α form. The amount of structural disorder decreases with increasing the crystallization temperature and the degree of stereoregularity of the samples. The presence of disorder in the crystals of γ form accounts for their lower melting temperature. This analysis indicates that metallocene isotactic polypropylene crystallizes in a continuum of disordered modifications intermediate between the α and γ forms, and the amount of disorder present in the crystals depends on the crystallization conditions and on the stereoregularity of the sample.

Introduction

With the development of metallocene catalytic systems for the isospecific polymerization of olefins, new isotactic polypropylenes (iPP) showing a wide variety of microstructures have become available. Depending on the specific metallocene complex used as catalyst, as well as on the polymerization conditions (i.e., monomer concentration, temperature, nature of cocatalyst, etc.), iPP samples containing different amounts and combinations of defects of stereoregularity (primary insertions with the wrong enantioface, or *stereodefects*) and regioregularity (meso and racemo secondary insertions, or *regiodefects*) can be obtained.[1]

The polymorphic behavior of these iPP samples, and, in particular, the relative stability of the α and γ forms under common conditions of crystallization, is completely different from that of iPP samples prepared with heterogeneous catalysts and is closely related to their microstructure.[2−8]

Commercial iPP, prepared with the traditional heterogeneous Ziegler−Natta catalytic systems, generally crystallizes in the stable α form.[9] The γ form may be obtained only under special conditions, i.e., by crystallization from the melt at elevated pressures (about 5000 atm)[9,10] or by crystallization at atmospheric pressure of low molecular weight samples[11] and of copolymers containing small amounts (in the range 5−20 mol %) of other olefins.[12]

iPP samples prepared with homogeneous metallocene catalysts crystallize more easily in the γ form, even at atmospheric pressure and for high molecular weight samples.[2−8] The different polymorphic behavior of iPP samples prepared with heterogeneous and homogeneous catalysts is related to the different type and distribution along the chains of insertion mistakes, that is, stereodefects and regiodefects, generated by the different kinds of catalytic systems. The distribution of defects, in turn, influences the average length of the crystallizable (fully isotactic) sequences.

The studies published so far have contributed to clarify the factors that induce the crystallization of the α and γ forms.[2−12] All the data indicate that when the fully isotactic sequences are very short, iPP crystallizes in the γ form, whereas very long regular isotactic sequences generally crystallize only in the α form. In the chains of iPP samples prepared with metallocene catalysts the distribution of defects is random, and the length of fully isotactic sequences is roughly inversely related to the content of insertion errors. As a consequence, even a small amount of defects reduces the length of the regular isotactic sequences and the γ form crystallizes.[2,5−8] In the case of iPP samples obtained with heterogeneous Ziegler−Natta catalytic systems, instead, the majority of the defects may be segregated in a small fraction of poorly crystallizable macromolecules, so that much longer, fully isotactic sequences can be produced, leading to the crystallization in the α form even for a relatively high overall concentration of defects.[9]

It has been shown that for iPP samples prepared with metallocene catalysts mixtures of the α and γ forms are generally obtained by isothermal crystallization from the melt,[2,5,6] and the content of the γ form increases with increasing content of defects.[2,6,8] In the extensive work of Alamo et al.,[2−4] the influence of the molecular weight and of the type and content of defects on the crystallization of the γ form has been investigated. The formation of the γ form seems to be favored by the presence of stereodefects (mainly *rr* isolated triads),[2] and/or regiodefects (mainly 2,1 and 3,1 insertions),[2,5] and also by the presence of constitutional defects, like comonomeric units.[4,6]

10.1021/ma020648r CCC: $22.00
Published on Web 10/17/2002

Table 1. Polymerization Temperatures (T_{pol}), Concentrations of the Pentad [*mmmm*] and the Dyad [*m*], Triads Distribution, Molecular Masses (M_w), Fractions of Stereoerrors (ϵ), Average Lengths of Fully Isotactic Sequences ($\langle L_{iso} \rangle$), and Melting Temperatures of the As-Prepared Powders (T_m) of the Three IPP Samples Prepared with the Highly Regiospecific *rac*-isopropyliden[bis(3-trimethylsilyl)(indenyl)]zirconium/MAO Catalytic System[17]

samples	T_{pol} (°C)	[*mmmm*] (%)	[*m*] (%)	[*mm*] (%)	[*mr*] (%)	[*rr*] (%)	M_w	ϵ (%)	$\langle L_{iso} \rangle$ (monomeric units)	T_m (°C)[a]
R1	20	89.0	95.5	93.3	4.4	2.3	110 000	2.3	43	144
R2	50	87.4	94.8	92.1	5.2	2.6	75 000	2.6	38	141
R3	60	83.4	93.1	89.7	6.9	3.4	66 000	3.4	29	137

[a] Melting temperature measured from DSC scans of the "as-prepared" samples (heating rate 10 °C/min).

The kind of distribution of defects along the polymer chains also influences the crystallization of the γ form. It has been recently shown[8] that in the case of stereoblock polypropylene, prepared with oscillating metallocene catalysts,[13−15] the amount of γ form which develops in the melt−crystallization procedures is much lower than that obtained for iPP samples having the same overall concentration of defects, but prepared with stereorigid metallocene catalysts, which produce a random distribution of defects.[8] This has been explained considering that in the stereoblock polypropylene most of the defects are segregated in stereoirregular (atactic), noncrystallizable, blocks, which alternate to more regular isotactic sequences, long enough to crystallize in the α form.[8] This result confirms that the γ form crystallizes when the fully isotactic sequences are very short.[2]

Several issues related to the formation of the γ form are, however, still not completely clarified. For instance, Alamo and VanderHart[3,4] have recently shown that in iPP samples from metallocene catalysts defects of stereoregularity, like isolated *rr* triads, regio 2,1 meso defects,[3] or even constitutional defects, like ethylene comonomeric units in copolymers of iPP with low amount of ethylene,[4,6] are included in the crystalline regions. Since these samples crystallize in mixtures of α and γ forms, it is not clear whether a preferential segregation of defects in the crystals of one of the two polymorphic forms occurs. In other words, it is still not clear which crystalline form, α or γ, is able to tolerate such defects at the lowest cost of energy and whether the defects, in turn, play a role in favoring the crystallization of one form over the other, besides the already mentioned effect of shortening the regular isotactic sequences.

Another important issue is the observation that the amount of γ form obtained by isothermal crystallizations from the melt first increases with increasing the crystallization temperature (T_c), reaches a maximum at a critical value of T_c, and then decreases for higher T_c.[2,6,8] This behavior seems to be quite general and does not depend on the amount and kind of defects or on their degree of segregation. In fact, also in the case of stereoblock polypropylene, the same result has been found.[8] Alamo et al.[2] have suggested that this behavior is related to the fact that the concentration of crystallizable sequences, i.e., those of length that equal or exceed the requirement for a nucleus of critical size, changes with the temperature. Moreover, the relative stability of the α and γ forms at different crystallization temperature, their stability in the presence of defects, and finally their different melting behavior, may play an important role. In ref 2 it has been also shown that the melting temperature of the crystals in the γ form is always 5−10 °C lower than that of the crystals of the α form. Since the crystal packing of the two forms is quite equivalent,[16] this may be due to the small size of the crystals in the γ form and/or to the presence of high degree of disorder in the γ crystals.

In this paper all these issues have been analyzed performing a detailed study of the structure, the polymorphic behavior, and the thermal behavior of different samples of iPP having different amounts of defects of stereoregularity, prepared with a highly regiospecific metallocene catalyst at different temperatures. The features in the X-ray diffraction profiles and the thermal behavior of the various samples have been interpreted on the basis of a disordered model of packing for the γ form, which implies the idea of crystallization of disordered modifications intermediate between the α and γ forms. It is worth noting that metallocene iPP samples analyzed so far always include regio 2,1, eventually 3,1 errors, besides the normal stereoirregularities (isolated *rr* triads).[2−6] Therefore, the samples here analyzed provide the first example of metallocene-made iPP not including regioerrors. It is suggested that the easy inclusion of *rr* triads in the crystals[3,7] possibly favors the formation of these disordered modifications in the γ domains. This analysis allows to establish a more unified view of the crystallization of metallocene iPP.

Experimental Section

Three samples of iPP, R1, R2, and R3, were synthesized at different temperatures using the single-center catalyst *rac*-isopropylidene[bis(3-trimethylsilylindenyl)]zirconium dichloride, activated with methylaluminoxane (MAO), as described in ref 17. This catalytic system is highly regiospecific and produces relatively high molecular weight iPP samples (the polydispersion index of the molecular masses is around 2) with a moderate stereoregularity and a random distribution of defects, mainly represented by isolated *rr* triads. The molecular weights, the melting temperatures, and the main microstructural characteristics of the three samples are reported in Table 1. The samples provide the first example of metallocene-made iPP not including regioerrors.

The samples were isothermally crystallized from the melt at different temperatures. Compression-molded specimens were melted at 180 °C and kept for 5 min at this temperature in a N_2 atmosphere; they were then rapidly cooled to the crystallization temperature, T_c, and kept at this temperature, still in a N_2 atmosphere, for a time t_c long enough to allow complete crystallization at T_c. The samples were then rapidly cooled to room temperature and analyzed by wide-angle X-ray diffraction. In the various isothermal crystallizations, the crystallization time t_c is different depending on the crystallization temperature. The shortest time is 24 h for the lowest crystallization temperatures and increases with increasing the crystallization temperature, up to 2 weeks for the highest crystallization temperatures.

X-ray powder diffraction patterns were obtained at room temperature with an automatic Philips diffractometer using Ni-filtered Cu Kα radiation and at higher temperatures using an attached Anton Paar TTK camera.

The calorimetric measurements were performed with a differential scanning calorimeter (DSC) Perkin-Elmer DSC-7 at different scan rates of 2.5, 10, 20, and 40 °C/min in a flowing N_2 atmosphere.

The relative amount of crystals in the γ form present in our samples was measured from the X-ray diffraction profiles, as suggested by Turner-Jones et al.,[18] by measuring the ratio between the intensities of the $(117)_\gamma$ reflection at $2\theta = 20.1°$, typical of the γ form, and the $(130)_\alpha$ reflection at $2\theta = 18.6°$, typical of the α form: $f_\gamma = I(117)_\gamma/[I(130)_\alpha + I(117)_\gamma]$. The intensities of $(117)_\gamma$ and $(130)_\alpha$ reflections were measured from the area of the corresponding diffraction peaks above the diffuse halo in the X-ray powder diffraction profiles. The amorphous halo has been obtained from the X-ray diffraction profile of an atactic polypropylene, and then it was scaled and subtracted from the X-ray diffraction profiles of the melt-crystallized samples.

Results and Discussion

X-ray Diffraction and Thermal Analysis. As already reported in ref 8, the samples R1, R2, and R3 (R*i* samples) of iPP crystallize from the melt in a mixture of crystals of the α and γ forms. The X-ray powder diffraction profiles of the as-prepared samples R*i* and of the samples isothermally crystallized from the melt at different temperatures, already reported in ref 8, are shown again in Figure 1. We recall that the α and γ forms of iPP present very similar X-ray diffraction profiles, the main difference being the position of the third strong diffraction peak, which occurs at $2\theta = 18.6°$ ($(130)_\alpha$ reflection) in the α form[19] and at $2\theta = 20.1°$ ($(117)_\gamma$ reflection) in the γ form.[20,21] The presence of the diffraction peak at $2\theta = 18.6°$ and the absence of the reflection at $2\theta = 20.1°$ in the X-ray diffraction patterns of the as-prepared R1 and R2 samples (profiles a in Figure 1, A and B, respectively) indicates that these samples are basically in the α form. The as-prepared powder of the less stereoregular sample R3 is instead crystallized in a mixture of crystals of the two forms of iPP, since both reflections of the α and γ forms are present in the X-ray diffraction profile (profile a in Figure 1C).

The diffraction patterns of the melt-crystallized samples present both $(130)_\alpha$ and $(117)_\gamma$ reflections, indicating that the γ form develops by crystallization from the melt. The relative intensity of the $(117)_\gamma$ reflection of the γ form at $2\theta = 20.1°$, with respect to that of the peak of the α form at $2\theta = 18.6°$ ($(130)_\alpha$ reflection), increases with increasing the crystallization temperature, reaches a maximum value, and then decreases for a further increase of the crystallization temperature. The relative amount of the γ form with respect to the α form, f_γ, for the various samples is reported in Figure 2 as a function of the crystallization temperature. The content of the γ form increases with increasing the crystallization temperature and a maximum amount is obtained, for each sample, at temperatures in the range 120−130 °C. Similar curves have already been reported and discussed in refs 2 and 6 for different samples of iPP prepared with different metallocene catalysts. As already observed in the literature,[2,6,8] the content of γ form increases with increasing the concentration of defects. The crystallization of the γ form is favored in iPP samples characterized by short regular isotactic sequences. The lower the degree of isotacticity, the higher is the maximum amount of the crystallized γ form (f_γ(max)). In particular, f_γ(max) ≈ 78% for the sample R1 ([*mmmm*] = 89.0%) and 90% for the less stereoregular samples R2 and R3 ([*mmmm*] = 87.4 and 83.4%, respectively).

The DSC curves, recorded at heating rate of 10 °C/min, of the melt-crystallized samples R1, R2, and R3

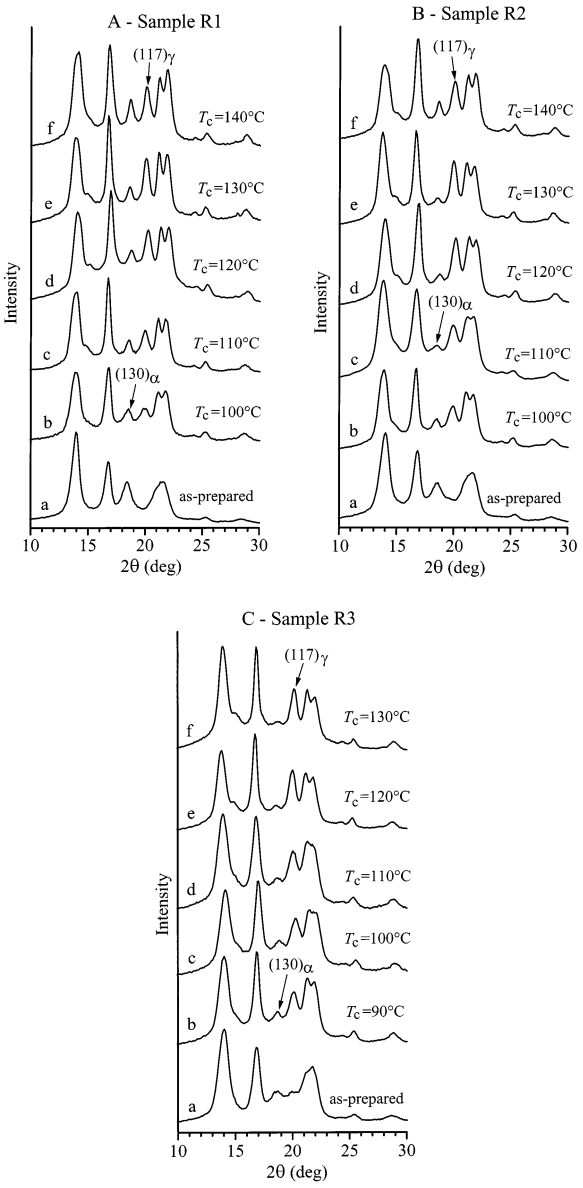

Figure 1. X-ray powder diffraction profiles of the as-prepared iPP samples and of specimens of the same samples isothermally crystallized form the melt at the indicated temperatures: (A) sample R1; (B) sample R2; (C) sample R3. The $(130)_\alpha$ and $(117)_\gamma$ reflections at $2\theta = 18.6°$ and 20.1°, respectively, typical of the α and γ forms of iPP, respectively, are also indicated.

are reported in Figures 3A, 4A, and 5A, respectively. All the samples show broad melting endotherms characterized by double peaks. The peak at lower temperature is present as a shoulder of the peak at higher temperature in the DSC scan of the samples crystallized at low temperatures (for instance, at $T_c = 100$ °C in Figures 3A and 4A and at $T_c = 90$ °C in Figure 5A). At higher crystallization temperatures the two peaks are well separated and clearly evident. For the three samples, the area of the peak at low temperature increases with increasing the crystallization temperature, up to $T_c = 130$ °C for samples R1 and R2 (curves d in Figures 3A and 4A) and $T_c = 120$ °C for sample R3 (curve d in Figure 5A), and then it decreases for a further increase of the crystallization temperature, as shown, for instance, for sample R1 in Figure 3A (curve e). Moreover, whereas the two peaks are separated by nearly 15 °C in the DSC scan of the samples crystallized

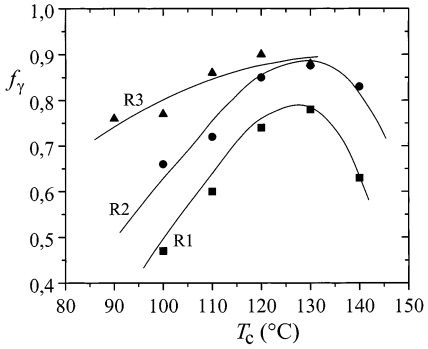

Figure 2. Content of the γ form of iPP, evaluated from the X-ray diffraction profiles, f_γ, in the samples isothermally crystallized from the melt, as a function of the crystallization temperature, T_c: (■) sample R1, [*mmmm*] = 89%; (●) sample R2, [*mmmm*] = 87.4%; (▲) sample R3, [*mmmm*] = 83.4%.

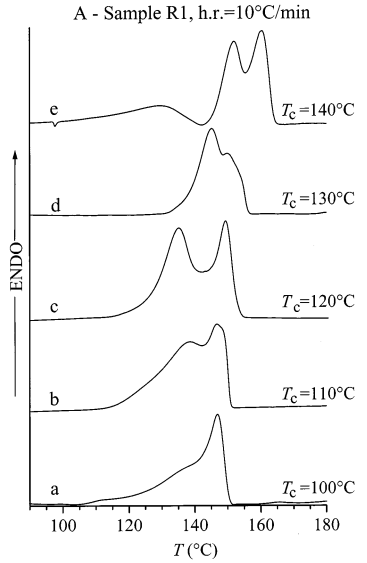

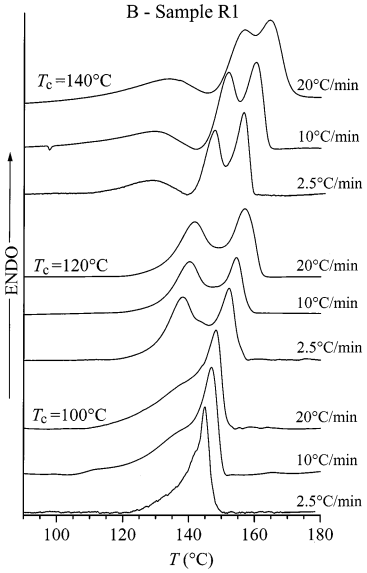

Figure 3. DSC curves at 10 °C/min of the samples R1 isothermally crystallized from the melt at the indicated temperatures (A). DSC curves at different heating rates of some samples R1 crystallized from the melt at the indicated temperatures (B).

at low temperatures (for instance at T_c = 120 °C, in Figure 3A), they approach each other at higher crystallization temperatures and are separated by less than 10 °C in the DSC scans of the samples crystallized, for instance at 140 °C (curve e in Figure 3A). This indicates that the materials crystallized at high crystallization temperatures melts in a more narrow range of temperatures.

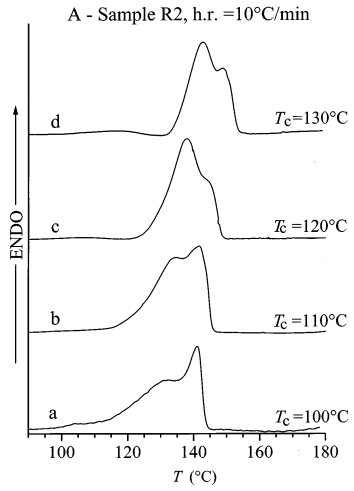

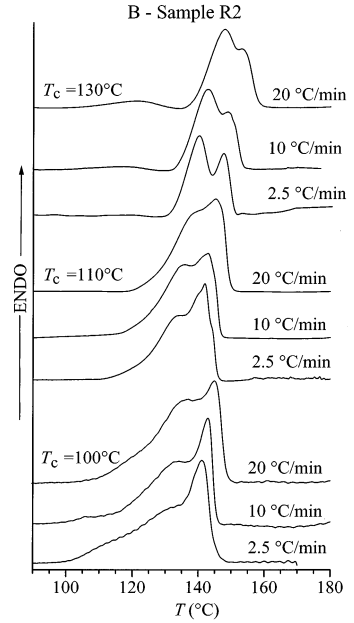

Figure 4. DSC curves at 10 °C/min of the samples R2 isothermally crystallized from the melt at the indicated temperatures (A). DSC curves at different heating rates of some samples R2 crystallized from the melt at the indicated temperatures (B).

In the case of samples crystallized at highest temperatures (for instance at 140 °C for sample R1) an additional broad endotherm is present at very low temperatures (in the range 120−130 °C) (curve e in Figure 3A). This is probably due to the melting of the material which does not crystallize at T_c, even for very long crystallization times, but crystallizes during the quenching to room temperature. The contribution of this endotherm to the global heat of melting is only 5−10% and cannot be further reduced by further increasing the crystallization time.

The melting behavior of metallocene iPP samples crystallized from the melt has been extensively studied by Alamo et al.[2] They have shown that the multiple peaks present in the DSC scans are due to the melting

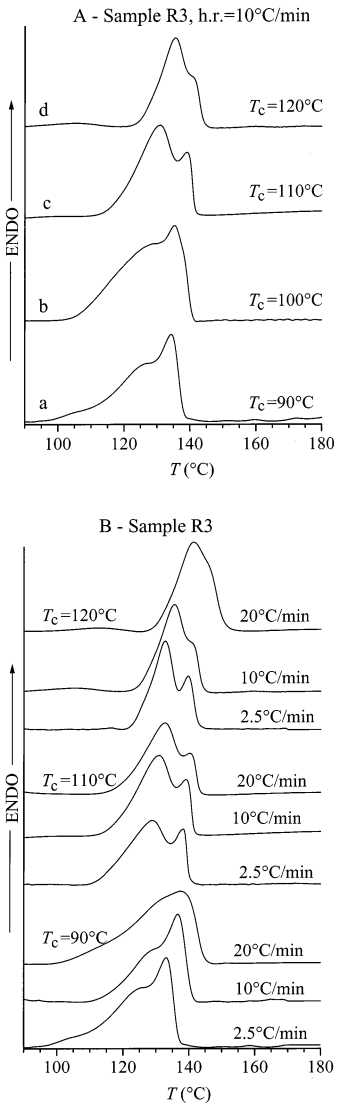

Figure 5. DSC curves at 10 °C/min of the samples R3 isothermally crystallized from the melt at the indicated temperatures (A). DSC curves at different heating rates of some samples R3 crystallized from the melt at the indicated temperatures (B).

of the two polymorphic forms of iPP.[2] The γ form melts, generally, at lower temperatures and, in some samples, shows two different melting peaks, which have been associated with different crystals of γ form having different morphologies,[2] also according to the atomic force microscopy observation.[5] These hypotheses could be valid also for our samples, which are characterized by mixtures of crystals of α and γ forms (Figure 1), even though the double peak shape of the endotherms in the DSC scans of Figures 3−5 could also be due, at least in part, to the occurrence of recrystallization phenomena during the heating. To analyze the possibility of recrystallization, DSC scans were performed at different heating rates (parts B of Figures 3−5). It is apparent from Figures 3B, 4B, and 5B that in all the DSC scans the relative areas of the two melting peaks do not change significantly by changing the heating rate. This indicates that the two melting peaks are not the result of the occurrence of recrystallization but are mostly due to the melting of the two crystalline polymorphs of iPP, even though the occurrence of not relevant recrystallization phenomena cannot be excluded.

This hypothesis has been confirmed by the X-ray diffraction patterns of the melt-crystallized samples recorded at different temperatures reported in Figure 6. For some selected melt-crystallized samples, the X-ray diffraction profiles have been recorded at room temperature and at temperatures corresponding to the onset of the melting endotherm and to the two peaks in the corresponding DSC curve. According to the results of Alamo et al.,[2] in all the analyzed samples, the X-ray diffraction profile remains unchanged from room temperature (profiles a in Figure 6) up to the temperature corresponding to the onset of the melting peaks (profiles b in Figure 6). In the X-ray diffraction patterns recorded at higher temperatures the intensities of the reflections of the γ form (mainly the $(117)_\gamma$ at $2\theta = 20.1°$) decrease progressively over a broad range of temperatures (as large as 15 °C) (profiles c in Figure 6). The reflections of the γ form disappear at temperatures higher than the first melting peak in the DSC scan, and for temperatures corresponding to the maximum of the second peak, only reflections of the α form are generally present in the X-ray diffraction patterns (profiles d in Figure 6). These data clearly indicate that, as already shown by Alamo et al.[2] for different iPP samples, the peak at low temperature in the melting endotherm corresponds basically to the melting of the γ form, while that at high temperature corresponds to the melting of crystals of the α form.

In the case of the samples crystallized at the highest temperatures, which present in the DSC scan an additional broad endotherm at low temperature, due to the melting of a fraction of the material crystallized during the quenching to room temperature (for instance, curve e in Figures 3A), the X-ray diffraction profile recorded at a temperature higher than that of this broad endotherm shows a reduction of the intensity of the reflection of the γ form. For instance, the case of the sample R1 crystallized at 140 °C is reported in Figure 6B. The X-ray diffraction profile recorded at 140 °C, between the broad low-temperature endotherm and the high-temperature double peak shaped endotherm, shows a reduction of the intensity of the $(117)_\gamma$ at $2\theta = 20.1°$ (profile b in Figure 6B) with respect to that in the X-ray diffraction pattern at room temperature (profile a in Figure 6B). This indicates that the fraction of material, which does not crystallize isothermally at the crystallization temperature but crystallizes during the quenching to room temperature, is basically in the γ form. Moreover, as also shown by Alamo et al.,[2] this demonstrates that the decrease of the content of γ form at high crystallization temperatures in the curves of Figure 2 is authentic and not an artifact due to the fact that a fraction of the material is unable to crystallize at the highest crystallization temperatures.

Once the two melting peaks in the DSC scans of the samples crystallized from the melt have been attributed to the melting of the α and γ crystals, it is possible to evaluate the content of γ form in these samples from the relative area of the peaks in the DSC scans: $f_{\gamma(\mathrm{DSC})} = \Delta H_\gamma/\Delta H_t$, where ΔH_γ is the area of the peak at low temperature and ΔH_t is the total enthalpy of melting. The values of the content of γ form so evaluated are reported in Figure 7 as a function of the crystallization temperature. The same behavior as that of the curves of Figure 2 is apparent. The content of γ form increases with increasing the crystallization temperature, reaches a maximum for T_c around 120−130 °C, and then

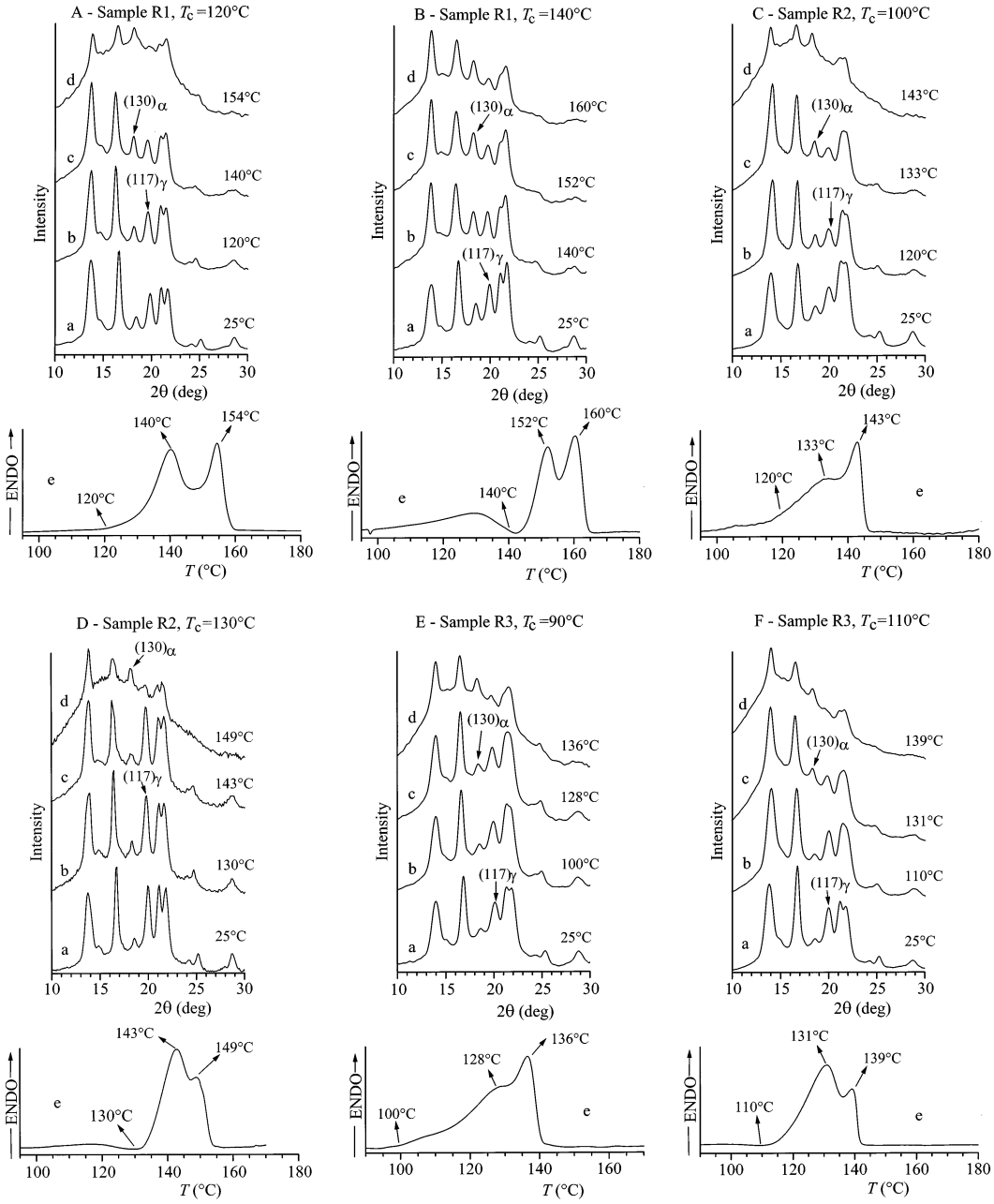

Figure 6. X-ray powder diffraction profiles of iPP samples isothermally crystallized form the melt recorded at 25 °C (a), at the temperature corresponding to the onset of the melting endotherm (b), and at temperatures corresponding to the two peaks of the melting endotherm (c, d). The corresponding DSC scan recorded at 10 °C/min is also shown (e). (A) sample R1 crystallized at T_c = 120 °C; (B) sample R1 crystallized at T_c = 140 °C; (C) sample R2 crystallized at T_c = 100 °C; (D) sample R2 crystallized at T_c = 130 °C; (E) sample R3 crystallized at T_c = 90 °C; (F) sample R3 crystallized at T_c = 110 °C. The $(130)_\alpha$ and $(117)_\gamma$ reflections at 2θ = 18.6° and 20.1°, respectively, typical of the α and γ forms of iPP, respectively, are also indicated.

decreases for further increase of T_c. As in Figure 2, the content of γ form increases with decreasing the degree of stereoregularity of the samples.

The crystallization of the R*i* samples has also been studied in nonisothermal conditions. The X-ray diffraction profiles of the sample R3 crystallized by cooling the melt at cooling rates of 40, 20, 10, 5, and 2.5 °C/min are reported in Figure 8 as an example. Also in this case the samples crystallize in mixtures of α and γ forms. Fast cooling rates favor the crystallization of the α form, whereas for slow cooling rates the crystallization of the γ form is favored. This is in agreement with results reported in the literature for other iPP samples.[22] The content of γ form, evaluated from the X-ray diffraction patterns of the kind shown in Figure 8, is reported in Figure 9 as a function of the cooling rate for all three samples. The extrapolation to zero cooling rate of the values of f_γ gives the maximum amounts of γ form, f_γ(max), which can be obtained for each sample in these conditions. These values nearly coincide with the maximum amount of γ form obtained by isothermal crystallization from the melt, deduced from the maxima of the curves of Figure 2.

The results of the present analysis indicate that samples of iPP prepared with metallocene catalysts crystallize from the melt in mixtures of crystals of α and γ forms. The crystals of the two polymorphic forms melt at different temperatures: the γ form at lower temperatures, the α form at higher temperatures. The melting temperature of both forms increases with increasing the

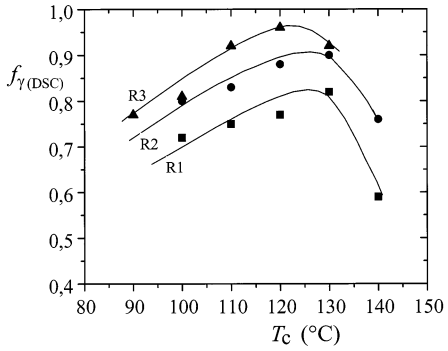

Figure 7. Content of the γ form of iPP, evaluated from the DSC curves of Figure 3, $f_{\gamma(DSC)}$, in the samples isothermally crystallized from the melt, as a function of the crystallization temperature T_c: (■) sample R1, [*mmmm*] = 89%; (●) sample R2, [*mmmm*] = 87.4%; (▲) sample R3, [*mmmm*] = 83.4%.

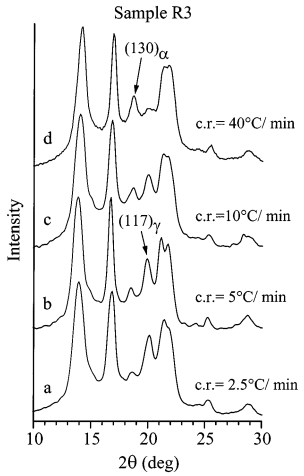

Figure 8. X-ray powder diffraction profiles of sample R3 crystallized form the melt by cooling to room temperature at the indicated cooling rates. The $(130)_\alpha$ and $(117)_\gamma$ reflections at $2\theta = 18.6°$ and 20.1°, respectively, typical of the α and γ forms of iPP, respectively, are also indicated.

crystallization temperature and the degree of stereoregularity. The γ form melts in a rather broad range of temperature (about 10 °C), which decreases with increasing the crystallization temperature, whereas the α form melts in a range of only 3 °C. This is probably due to the fact that the crystals of γ form present a high degree of structural disorder,[7] as we will discuss in the next section, and/or include a large amount of defects. The crystals of the α form are, instead, probably more perfect and also of larger dimension and melt at higher temperatures and in a narrower range of temperature. In the next section the crystal structure of these melt-crystallized iPP samples, and the possible presence of structural disorder, are analyzed in detail through the comparison of the X-ray powder diffraction profiles of Figure 1 with the diffraction profiles calculated for models of structure which include mixtures of α and γ forms and disorder in the regular packing of the chains.

Model of Disordered Structures and Method of Calculation of the X-ray Diffraction Patterns

A comparison between the modes of packing of the chains in the α and γ forms is reported in Figure 10. In both forms chains in 3/1 helical conformations are organized in double layers. In the α form (Figure 10B), the bilayers are piled along the crystallographic b_α direction with all chain axes parallel to each other.[19] In the γ form (Figure 10A), the bilayers are piled along the c_γ direction, and the chain axes in adjacent bilayers are nearly perpendicular to each other (tilted by 81°).[20,21]

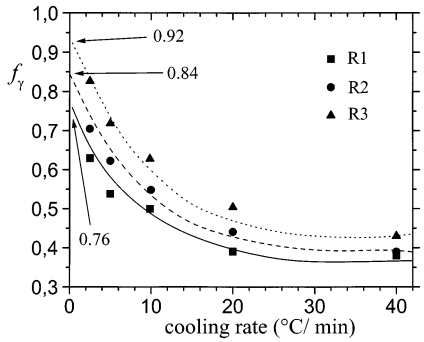

Figure 9. Content of the γ form of iPP, evaluated from the X-ray diffraction profiles of the kind shown in Figure 8, f_γ, in the R*i* samples crystallized from the melt by cooling to room temperature at different cooling rates, as a function of the cooling rate. The maximum amounts of the γ form obtained by extrapolation to zero cooling rate are also indicated. (■) sample R1, [*mmmm*] = 89%; (●) sample R2, [*mmmm*] = 87.4%; (▲) sample R3, [*mmmm*] = 83.4%.

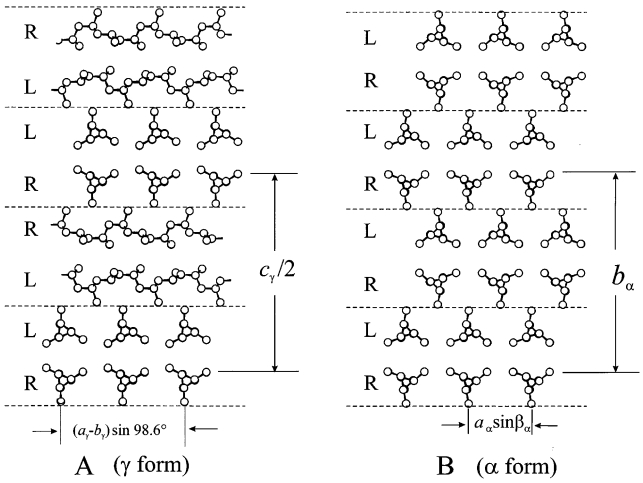

Figure 10. Models of packing proposed for the γ (A) and the α (B) forms of iPP. The dashed horizontal lines delimit bilayers of chains. Subscripts α and γ identify unit cell parameters referred to the monoclinic and orthorhombic unit cells of the α and γ forms, respectively. R and L identify rows of all right- and all left-handed helices, respectively.

In a recent paper we have shown that a low stereoregular iPP sample crystallizes by stretching in disordered modifications of iPP.[7] Pure α and γ forms were never obtained, but only disordered modifications intermediate between the α and γ forms, with structures close to the α or γ forms depending on the draw ratio, were obtained.[7] The proposed model of disorder is shown in Figure 11. Consecutive bilayers of chains may face each other with the chain axes either parallel (like in the α form) or nearly perpendicular (like in the γ form) (Figure 11). Two adjacent bilayers have chains parallel each other with a probability p_α or nearly perpendicular with a probability $p_\gamma = 1 - p_\alpha$. In this model of disordered structure, ordered domains in the α or γ forms are present inside the same crystal, giving rise to a mixture at molecular level of the α and γ forms (Figure 11). In the ref 7 we have shown that, different disordered modifications, containing different amounts of α-like or γ-like arrangements of the chains, depending on the draw ratio, can be obtained.

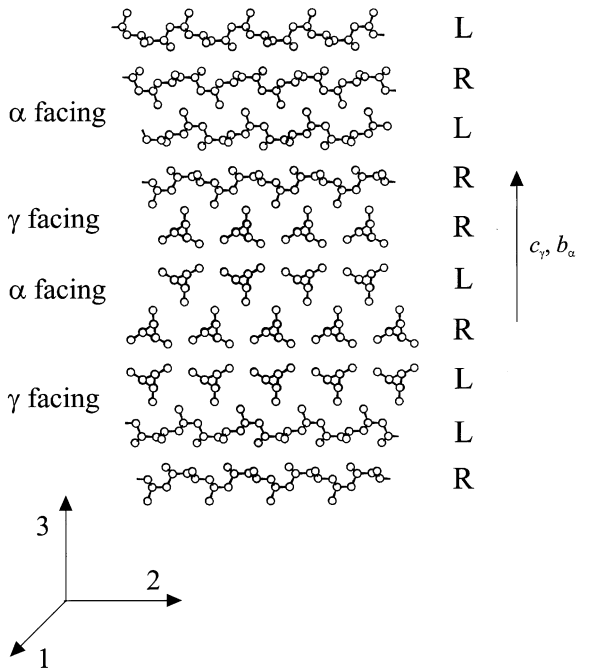

Figure 11. Model of the α/γ disorder occurring in the disordered modifications of iPP intermediate between the α and γ forms. Consecutive $a_\alpha c_\alpha$ ($a_\gamma b_\gamma$) bilayers of chains are stacked along b_α (c_γ) with the chain axes either parallel or nearly perpendicular, making α-like or γ-like arrangements of the bilayers. R and L identify rows of all right- and all left-handed chains, respectively. The three lattice directions 1, 2, and 3 are indicated.

We believe that the same kind of structural disorder may also be present in the samples isothermally crystallized from the melt reported in this paper, because a simple mixture of crystals of the pure α and γ forms does not account for the intensities of the reflections in the X-ray powder diffraction patterns of Figure 1. In these patterns, indeed, the intensities of the $(110)_\alpha$ (or $(111)_\gamma$), $(130)_\alpha$, and $(117)_\gamma$ reflections at $2\theta = 14°$, 18.6°, and 20.1°, respectively, are generally lower than those expected by the diffraction of separate crystals of pure α and γ forms. In some patterns the $(130)_\alpha$ and $(117)_\gamma$ reflections are almost absent (for instance the pattern a of Figure 1C), and only a diffuse scattering is instead observed in the corresponding 2θ range. The experimental observations cannot be explained by a mixture of α and γ crystals. As shown in ref 7, the presence of α/γ disorder in the crystalline domains, of the kind of Figure 11, induces fluctuations in the relative intensities of the Bragg peaks and introduces some diffuse scattering. The diffuse scattering concentrates in very narrow regions of the diffraction diagrams, i.e., mainly around $2\theta \approx 14°$ (reflections $(110)_\alpha$ and $(111)_\gamma$), in the 2θ range 18−20° (where the reflections $(130)_\alpha$ and $(117)_\gamma$ occur), and around $2\theta \approx 21.9°$ (reflections $(\bar{1}31)_\alpha$ and $(026)_\gamma$). Moreover, the intensities and the positions of other strong reflections, such as the $(040)_\alpha$ or $(008)_\gamma$ ($2\theta \approx 17°$) and the $(111)_\alpha$ or $(202)_\gamma$ ($2\theta \approx 21.1°$), are not affected by the presence of disorder and/or by the relative amounts of the α and γ phases present in a given sample. Therefore, the presence of this kind of disorder would reduce the intensities of the $(110)_\alpha$, $(111)_\gamma$, $(130)_\alpha$, and $(117)_\gamma$ reflections, whereas the $(040)_\alpha$ or $(008)_\gamma$ and the $(111)_\alpha$ or $(202)_\gamma$ reflections would remain strong and sharp, according to the experimental observations. We have performed a quantitative analysis through a direct comparison of the experimental X-ray diffraction data with those calculated for suitable model structures.

We have calculated the X-ray powder diffraction profiles for models of structure of the kind of Figure 11, including variable amounts of α/γ disorder, and compared the experimental X-ray diffraction pattern of the samples crystallized from the melt at different temperatures (Figure 1) to the calculated profiles.

The method of calculation has already been described in the ref 7, in the case of oriented iPP samples. In this paper, instead, we calculate the diffraction profiles of unoriented powder samples; therefore, the calculated intensity (I_c) is evaluated by integrating the intensity function $I(s,\rho,\varphi)$ in the reciprocal space over surfaces with radius equal to the modulus of the reciprocal scattering vector **s**, $|\mathbf{s}| = 2 \sin\theta/\lambda$, where ρ and φ are the spherical polar reciprocal coordinates, ρ the angle between **s** and the z axis of a reference frame, and φ the angle between the projection of **s** in the a^*-b^* plane and the a^* axis. The surface integral is given by the equation

$$I_c = \frac{1}{4\pi}\int_0^{\pi} \sin\rho \, d\rho \int_0^{2\pi} I(s,\rho,\varphi) \, d\varphi \qquad (1)$$

The intensity function $I(s,\rho,\varphi)$ is evaluated according to eq 2 of ref 7. With reference to the three lattice directions 1, 2, and 3 shown in Figure 11, we have defined in ref 7 bilayers of kinds 1 or 2 as bilayers with chains having their axes along the directions 1 or 2, respectively (Figure 11). The conditional probabilities p_{ij} ($i, j = 1, 2$) were defined in ref 7 as the probabilities that a bilayer of kind i is followed along the direction 3 by a bilayer of kind j. At the interface of adjacent bilayers, local arrangements of the chains like in the α or γ forms are obtained for $i = j$ or $i \neq j$, respectively. The regular stacking of bilayers of kind 1 (or 2) along the direction 3 gives rise to ordered domains with the chains packed like in the α form, all the chain axes being parallel ($p_{11} = 1$, or $p_{22} = 1$). The regular alternation of bilayers of kind 1 and 2, instead, gives rise to domains ordered like in the γ form of iPP ($p_{12} = p_{21} = 1$). Since in this paper we calculate the powder diffraction profiles, no preferred orientations of the chains are considered; therefore, the distribution of the X-ray diffraction intensity depends on a single parameter, i.e., the relative amount of α-like or γ-like arrangements of adjacent bilayers, p_α or p_γ, respectively, with $p_\alpha + p_\gamma = 1$. Hence, with respect to ref 7, the calculation is simplified assuming $p_{ii} = p_{jj} = p_\alpha$ and $p_{ij} = p_{ji} = p_\gamma$.

The structure factors of the bilayers of the kinds 1 and 2, V_1 and V_2, respectively, are calculated using the fractional coordinates of the atoms in the bilayers deduced from those reported in the ref 20. In the calculations, the presence of up/down disorder is assumed;[19,20] therefore, the structure factors V_1 and V_2 are average values, evaluated assuming that each site of the lattice is occupied by up and down chains with the same probability. A Bernoullian distribution of the size of the crystallites along the directions 1, 2, and 3 is assumed,[23] L_1, L_2, and L_3 being the apparent average lengths of the crystallites along the three directions 1, 2, and 3, respectively.

According to the suggestions obtained from the experimental X-ray diffraction and melting behavior analyses, the calculations of the powder diffraction profiles were performed in the hypothesis that in the samples two crystalline phases are present, crystals in

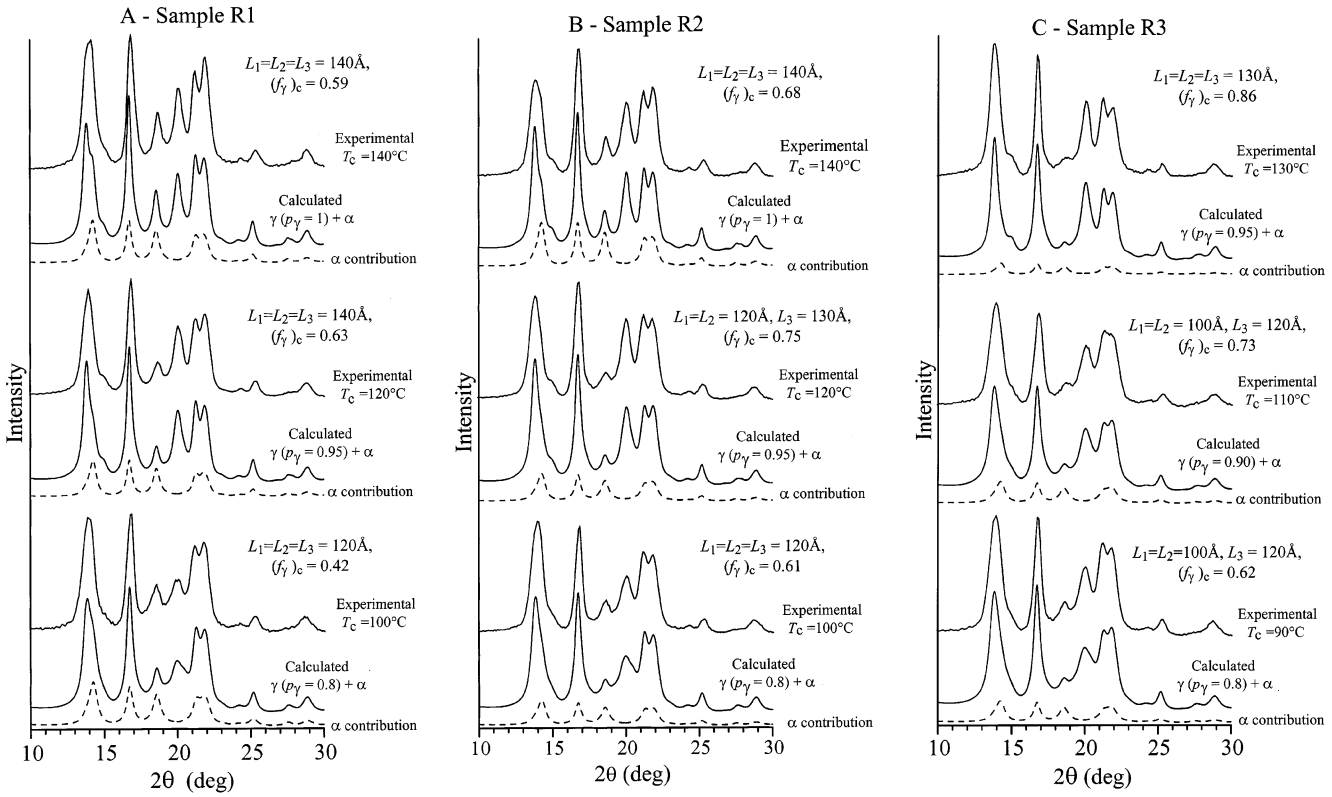

Figure 12. Comparison between some experimental X-ray powder diffraction profiles of Figure 1 of the iPP samples isothermally crystallized from the melt at the indicated temperatures, after the subtraction of the amorphous halo and the correction for the polarization factor (upper profiles), and calculated X-ray diffraction profiles, which give the best agreement with the experimental profiles (lower profiles). The X-ray diffraction profiles are calculated for mixtures of crystals in the pure α form and in defective γ form, containing different amounts of α/γ disorder (like in the model of Figure 11). For each calculated profile the contribution of the diffraction of crystals in the pure α form is also shown as dashed profile. The amount of disorder in the model of disordered γ form (like the model of Figure 11) is indicated by the values of p_γ. The fraction of γ form in the calculated profiles is also indicated as $(f_\gamma)_c$. The values of the average size of the crystallites L_1, L_2, and L_3 used in the calculated profiles are also shown. (A) sample R1; (B) sample R2; (C) sample R3.

the pure α form and crystals in the γ form, the latter eventually containing different amounts of α/γ disorder. For the sake of simplicity, the apparent size of the crystallites was assumed equal for the two crystalline phases. In particular, the value of L_3 was deduced, applying the Scherrer's formula, from the half-height width of the $(008)_\gamma$ reflection (for the γ form) and $(040)_\alpha$ reflection (for the α form) at $2\theta = 17°$ in the experimental X-ray powder diffraction profiles of Figure 1. The values of L_1 (assumed equal to L_2 in all the calculations) have been deduced from the half-height width of the equatorial reflections, $(110)_\alpha$ and $(130)_\alpha$ for the α form and $(111)_\gamma$ and $(117)_\gamma$ for the γ form.

The above assumptions are quite reasonable and highly consistent with the results of some kinetic, morphological, and SAXS studies on Ziegler−Natta iPP samples melt crystallized at high pressures[24,29] and on metallocene-made iPP samples, melt crystallized at atmospheric pressure.[2,5] During the crystallization from the melt, α and γ crystals form almost simultaneously since the early stages.[2,25] The α and γ lamellae show the helical stems inclined about 50° with respect to the lamella surface. Moreover, α and γ lamellae do not exist as isolated, independent entities.[24] In these systems indeed, the γ lamellae have been observed to form stacks of lamellae branched off the α lamellae.[30] Branched lamellae and mother lamellae correspond to a same thickness and give rise to a variety of structures, i.e., spherulites[5,24,25,29] and elongated and bundle-like entities.[5] Therefore, as observed in ref 24, the stem lengths of the α and γ phase obtained in the same conditions of pressure and temperature are close to one another. This correspond to assume that the α and γ population of crystals have the same average dimensions along directions 1 and 2 of Figure 11, coinciding with the c_α and a_α lattice directions for α crystals, respectively, to the diagonal lattice directions for the γ crystals.

Results of the Calculations

Some experimental X-ray powder diffraction profiles of Figure 1 of the samples R*i* isothermally crystallized from the melt at different temperatures are reported in Figure 12 after the subtraction of the amorphous halo and the correction for the polarization factor. The calculated profiles, which give the best agreement with the experimental profiles, are also shown in Figure 12. The X-ray diffraction profiles are calculated for mixtures of α and γ forms and for different amounts of α/γ disorder present in the crystals of the γ form. Each calculated profile is, therefore, the sum of the contribution of the diffraction of crystals in the pure α form (also shown in Figure 12 as dashed profiles) and the contribution of the diffraction of disordered crystals of the γ form, containing a suitable amount of α/γ disorder (like in the model of Figure 11). The amount of disorder is indicated by the values of the probability p_γ. The values of the average size of the crystallites used in the calculations are also indicated in Figure 12. For each sample R*i*, the size of the crystallites increases with

increasing the crystallization temperature, being in all cases of the order of 100−140 Å.

It is apparent from Figure 12 that, for all the samples crystallized from the melt, disorder in the crystals of the γ form is almost always present. The amount of structural disorder in the γ form decreases with increasing the crystallization temperature; it corresponds to the presence of 20% of α-like arrangements of the chains in the samples crystallized at low temperatures (i.e., $p_\gamma = 0.8$, $p_\alpha = 1 - p_\gamma = 0.2$ for the samples R1 and R2 crystallized at $T_c = 100$ °C in parts A and B of Figure 12, respectively, and for the sample R3 at $T_c = 90$ °C in Figure 12C) and decreases to only 5% of α-like arrangements in the samples crystallized at higher temperatures (i.e., $p_\gamma = 0.95$, $p_\alpha = 1 - p_\gamma = 0.05$ for the samples R1 and R2 at $T_c = 120$ °C in parts A and B of Figure 12, respectively, and for the sample R3 at $T_c = 130$ °C in Figure 12C). It is worth noting that for the most stereoregular samples R1 and R2 the disorder in the γ form is basically absent in the samples crystallized at the highest temperature ($p_\gamma = 1$ at $T_c = 140$ °C in Figure 12A,B), whereas for the less stereoregular sample R3, disorder is always present even at the highest crystallization temperature ($p_\gamma = 0.95$ at $T_c = 130$ °C in Figure 12C). Moreover, it is also worth noting that the contribution of the crystals in the pure α form (dashed profiles in Figure 12) is very small (about 10%) for the less stereoregular samples R3 (Figure 12C), whereas it is higher for the most stereoregular samples R1 (Figure 12A).

The presence of disorder in the γ form, shown by the calculations, is in agreement with the experimental observations that the crystals of the γ form, obtained by crystallization from the melt, melt at lower temperatures and in a wider range than the crystals of the α modification formed at the same crystallization temperature (Figures 3−5). Moreover, the reduction of the amount of disorder with increasing the crystallization temperature (Figure 12) accounts for the larger increase of the melting temperature of the γ form than that of the α form with increasing the crystallization temperature (Figures 3−5).

Since the calculated profiles of Figure 12, which fit the experimental profiles of the melt-crystallized samples, are characterized by the sum of the contributions of the α and γ crystals, the calculated content of the γ form may be evaluated from the ratio between the area of the calculated profile giving the contribution of the γ form (A_γ) and the area of the whole calculated profile (A), A_γ/A. This parameter basically corresponds to that used for the evaluation of the γ content in the experimental profiles, f_γ, through the method suggested by Turner-Jones[18] and described in the Experimental Part. Since in our model the crystals of the γ form contain structural α/γ disorder, which introduces some variable amount of α-like arrangements of the chains, the contribution due to the diffraction of these disordered crystals (A_γ) does not give the correct amount of γ-like arrangements of the chains in the crystals. The real fraction of γ-like arrangements, $(f_\gamma)_c$, may be evaluated by multiplying the contribution due to the diffraction of the disordered crystals of the γ form (A_γ) by the order parameter p_γ, $(f_\gamma)_c = p_\gamma A_\gamma/A$. The values of $(f_\gamma)_c$ calculated for the three samples are reported in Figure 13 as a function of the crystallization temperature. The calculated curves of Figure 13 are similar to those of Figure 2, evaluated from the experimental X-ray diffraction patterns in the approximation of the method of Turner-Jones.[18] The values of $(f_\gamma)_c$ are slightly lower than those of f_γ of Figure 2, indicating that the content of γ form evaluated with the method of Turner-Jones is an upper limit of the effective γ-like arrangements present in our samples.

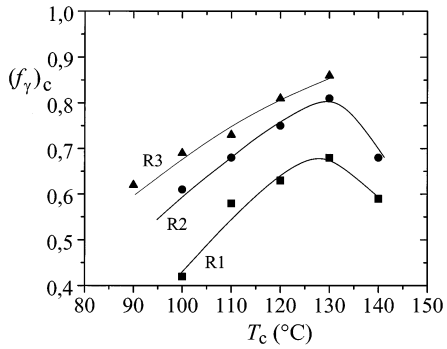

Figure 13. Calculated content of the γ form of iPP, evaluated from the calculated X-ray diffraction profiles of Figure 12, $(f_\gamma)_c$, for the samples isothermally crystallized from the melt, as a function of the crystallization temperature T_c. (■) sample R1, [*mmmm*] = 89%; (●) sample R2, [*mmmm*] = 87.4%; (▲) sample R3, [*mmmm*] = 83.4%.

It is worth mentioning that the presence of disordered modifications intermediate between the α and the γ forms of iPP was already hypothesized by Campbell et al.[24] on the basis of morphological observations and small-angle X-ray scattering (SAXS) experiments on Ziegler−Natta iPP samples crystallized from the melt at elevated pressures. In ref 24 it was observed that the coexistence and the concurrent growth of α and γ lamellae at the same temperature and pressure occur since the early stages of the crystallization; small-angle experiments, not showing any evidence for a bimodal population of lamellar thickness, indicated that the α and γ lamellae do not exist in identifiable separate stacks even at pressures where the amount of α crystals is small. On the other hand, the observed linear dependence of the relative amount of γ form with the pressure induced the authors of ref 24 to suggest the hypothesis that both crystal forms are present in each lamella, rather than existing as separate lamellae, giving rise to disordered modifications intermediate between the α and the γ form.

Conclusions

Samples of iPP prepared with metallocene catalysts crystallize from the melt in mixtures of crystals of α and γ forms. The content of the γ form increases with decreasing degree of stereoregularity of the samples. The crystals of the γ form melt at temperatures lower than those of the α form crystallized at the same temperature. The melting temperature of both forms increases with increasing crystallization temperature and degree of stereoregularity. The γ form melts in a rather broad range of temperatures (about 10 °C), which decreases with increasing crystallization temperature.

The comparison between calculated and experimental X-ray diffraction profiles has indicated that a simple mixture of crystals of α and γ forms does not account for the X-ray powder diffraction patterns. Crystals of the γ form obtained in these samples always present structural disorder, characterized by defects in the regular packing of bilayers of chains with axes oriented alternatively along two nearly perpendicular directions.

This disorder produces a local situation of packing typical of the α form, with some adjacent bilayers having parallel chains. The amount of structural disorder decreases with increasing crystallization temperature and degree of stereoregularity of the sample. The presence of disorder in the crystals of γ form accounts for their lower melting temperature. The results of our calculations indicate that the length of the crystallites along the chain axes (i.e., L_1 and L_2), assumed equal for both the populations of α and γ crystals, are in the range 100−140 Å and increase with the decrease of the amount of stereoirregularities and the increase of crystallization temperature. Considering that the helices in the α and γ crystals produced in these systems form an angle of about 50° with respect to the lamella surface,[4,25,26] the lamellar thickness of our samples corresponds to 80−110 Å, in good agreement with the results of recent studies on Ziegler−Natta iPP crystallized at elevated pressure.[25,26,29]

This analysis indicates that iPP prepared with metallocene catalysts crystallizes in a continuum of disordered modifications intermediate between the α and γ forms, the amount of disorder being dependent on the crystallization conditions and on the stereoregularity of the sample.

The crystallinity of the analyzed samples is always high (60−65%) regardless of the crystallization temperature and the amount of defects. This is probably due to the fact that some stereodefects can be included in the crystalline phase. For instance, isolated *rr* triads are defects possibly included in the crystals at a low cost of conformational and packing energy, as shown in ref 7 and demonstrated in ref 3 by accurate NMR experiments. Probably these defects are better tolerated in the crystals of the γ form than in those of the α form, and as shown in ref 7, their inclusion in the crystals may induce, itself, the α/γ structural disorder.

On the basis of this complex polymorphic behavior of iPP prepared with metallocene catalysts, the reason for the presence of maxima in the curves of the content of γ form as a function of the crystallization temperature may be explained as a result of two competing kinetic and thermodynamic effects. For the present samples of iPP, containing an appreciable amount of stereodefects, the formation of the γ form is thermodynamically favored, since the *rr* defects (the only one present in these samples) and the α/γ structural disorder are highly tolerated in the γ form, less in the crystals of the α form. As a consequence, a high amount of γ form develops in the slow crystallizations at high temperatures. At lower crystallization temperatures the fast crystallization of the α form is instead kinetically favored, giving a low amount of γ form. With increasing crystallization temperature the amount of γ form increases, but at very high crystallization temperatures (higher than 130 °C) the crystallization of the defective γ form is too slow because of its lower melting temperature, and the more perfect α form becomes again kinetically favored, so that the amount of γ form decreases.

Mezghani and Phillips reported important works concerning the phase diagram of iPP and the equilibrium melting point of the γ phase.[26] The two polymorphs have nearly the same thermodynamic stability, in agreement with the packing energy calculations of Ferro et al.[16] In ref 26, the temperature of transition between the α and γ form (in the limit of a system of infinite chain length and free of defects, forming infinite dimensions crystals) was also evaluated, and the polymorphic behavior of a commercial iPP sample, prepared via traditional heterogeneous Ziegler−Natta catalytic systems, was discussed in terms of the established phase diagram. In agreement with the thermodynamic predictions, the pure γ form can be obtained only at pressures higher than 100 MPa and low undercooling, whereas for pressures lower than 25 MPa, only the α form is obtained. In a large region of the phase diagram, however, i.e., at low pressure and high undercooling, for conditions where only the α form would be expected to form, both forms are found to be present. These deviations from the ideal were attributed to the heterogeneous nature of Ziegler−Natta systems: in these systems, chains or a portion of chains with a higher content of defects than the average fraction, favor the γ phase under conditions where the average molecule produce α crystals. Also, a phase transition between the two polymorphs has never been observed so far, probably because of kinetic reasons.[26] Metallocene-made iPP samples represent a more homogeneous system from this point of view (not generally fractionable), yet heterogeneous since, in the limit of a random distribution of errors, the distribution of the length of fully isotactic sequence L_{iso} is broad ($\langle L_{iso}^2\rangle/\langle L_{iso}\rangle = 2$) and becomes progressively more flat the higher the average value ($\langle L_{iso}\rangle$). Therefore, these systems generally produce mixtures of α and γ crystals upon melt crystallization procedures for the same reasons stated for Ziegler−Natta iPP systems in ref 26; i.e., long stems of fully isotactic sequences crystallize in the α form, and shorter ones containing a major number of defects are unable to crystallize in the α modification at that temperature and hence give the γ form. The α crystals produced by such short portions of chains would be, indeed, thermodynamically unstable because of the too short lamellar thickness. Moreover, the thickness cannot increase, for instance, by inclusions of defects in the crystals because the inclusion of (*rr*) defects in the α crystals is not easy and not compatible with the maintaining of the parallelism of the helical chains.[7] In other words, the short isotactic sequences crystallize in the γ form because in the γ crystals the inclusion of "punctual" defects, as for instance isolated *rr* triads,[7] and "planar" defects, as for instance α/γ stacking fault disorder of the kind shown in Figure 11, is at a low cost of packing and conformational energy and entropically favored.

Acknowledgment. We thank Dr. L. Resconi of Basell Poliolefine Italia for providing and selecting the three iPP samples and for having stimulated this study. Financial support from the "Ministero dell'Università e della Ricerca Scientifica e Tecnologica" (PRIN 2000 and Cluster C26 projects) is gratefully acknowledged.

References and Notes

(1) Resconi, L.; Cavallo, L.; Fait, A.; Piemontesi, F. *Chem. Rev.* **2000**, *100*, 1253.
(2) Alamo, R. G.; Kim, M. H.; Galante, M. J.; Isasi, J. R.; Mandelkern, L. *Macromolecules* **1999**, *32*, 4050.
(3) VanderHart, D. L.; Alamo, R. G.; Nyden, M. R.; Kim, M. H.; Mandelkern, L. *Macromolecules* **2000**, *33*, 6078.
(4) Alamo, R. G.; VanderHart, D. L.; Nyden, M. R.; Mandelkern, L. *Macromolecules* **2000**, *33*, 6094.
(5) Thomann, R.; Wang, C.; Kressler, J.; Mulhaupt, R. *Macromolecules* **1996**, *29*, 8425.
(6) Thomann, R.; Semke, H.; Maier, R. D.; Thomann, Y.; Scherble, J.; Mulhaupt, R.; Kressler, J. *Polymer* **2001**, *42*, 4597.

(7) Auriemma, F.; De Rosa, C.; Boscato, T.; Corradini, P. *Macromolecules* **2001**, *34*, 4815.
(8) De Rosa, C.; Auriemma, F.; Circelli, T.; Waymouth, R. M. *Macromolecules* **2002**, *35*, 3622.
(9) Brückner, S.; Meille, S. V.; Petraccone, V.; Pirozzi, B. *Prog. Polym. Sci.* **1991**, *16*, 361.
(10) Kardos, J. L.; Christiansen, W.; Baer, E. *J. Polym. Sci.* **1966**, *A-2* (4), 777. Pae, K. D.; Morrow, D. R.; Sauer, J. A. *Nature (London)* **1966**, *211*, 514. Pae, K. D. *J. Polym. Sci.* **1968**, *A-2* (6), 657. Sauer, J. A.; Pae, K. D. *J. Appl. Phys.* **1968**, *39*, 4959. Morrow, D. R. *J. Macromol. Sci., Phys. Ed.* **1969**, *B3*, 53.
(11) Lotz, B.; Graff, S.; Wittmann, J. C. *J. Polym. Sci., Polym. Phys.* **1986**, *24*, 2017. Kojima, M. *J. Polym. Sci.* **1967**, *5*, 245. Kojima, M. *J. Polym. Sci.* **1968**, *A-2* (6), 1255. Morrow, D. R.; Newman, B. A. *J. Appl. Phys.* **1968**, *39*, 4944.
(12) Turner-Jones, A. *Polymer* **1971**, *12*, 487.
(13) Coates, G.; Waymouth, R. M. *Science* **1995**, *267*, 217.
(14) Hu, Y.; Krejchi, M. T.; Shah, C. D.; Myers, C. L.; Waymouth, R. M. *Macromolecules* **1998**, *31*, 6908.
(15) Witte, P.; Lal, T. K.; Waymouth, R. M. *Organometallics* **1999**, *18*, 4147.
(16) Ferro, D. R.; Brückner, S.; Meille, S. V.; Ragazzi, M. *Macromolecules* **1992**, *25*, 523.
(17) Resconi, L.; Piemontesi, F.; Camurati, I.; Sudmeijer, O.; Ninfant'ev, I. E.; Ivchenko, K. V.; Kuz'mina, L. *J. Am. Chem. Soc.* **1998**, *120*, 2308.
(18) Turner-Jones, A.; Aizlewood, J. M.; Beckett, D. R. *Makromol. Chem.* **1964**, *75*, 134.
(19) Natta, G.; Corradini, P. *Nuovo Cimento Suppl.* **1960**, *15*, 40.
(20) Brückner, S.; Meille, S. V. *Nature (London)* **1989**, *340*, 455.
(21) Meille, S. V.; Brückner, S.; Porzio, W. *Macromolecules* **1990**, *23*, 4114.
(22) Perez, E.; Zucchi, D.; Sacchi, M. C.; Forlini, F.; Bello, A. *Polymer* **1998**, *40*, 675.
(23) Allegra, G.; Bassi, I. W. *Gazz. Chim. Ital.* **1980**, *110*, 437.
(24) Campbell, R. A.; Phillips, P. J.; Lin, J. S. *Polymer* **1993**, *34*, 4809.
(25) Mezghani, K.; Phillips, P. J. *Polymer* **1997**, *38*, 5725.
(26) Mezghani, K.; Phillips, P. J. *Polymer* **1998**, *39*, 3735.
(27) Meille, S. V.; Phillips, P. J.; Mezghani, K.; Brückner, S. *Macromolecules* **1996**, *29*, 795.
(28) Brückner, S.; Phillips, P. J.; Mezghani, K.; Meille, S. V. *Macromol. Rapid Commun.* **1997**, *18*, 1.
(29) Angelloz, C.; Fulchiron, R.; Damillard, A.; Chabert, B.; Fillit, R.; Vautrin, A.; David, L. *Macromolecules* **2000**, *33*, 4138.
(30) Lotz, B.; Graff, S.; Straupe, C.; Wittmann, J. C. *Polymer* **1991**, *32*, 2902.

MA020648R